Impact of information on quantum heat engines

Lindsay Bassman Oftelie and Michele Campisi
Istituto Nanoscienze–Consiglio Nazionale delle Ricerche, NEST Scuola Normale Superiore, 56127 Pisa, Italy

(Received 15 December 2025; accepted 4 May 2026; published 26 May 2026)

The emerging field of quantum thermodynamics is beginning to reveal the intriguing role that information can play in quantum thermal engines. Information enters as a resource when considering feedback-controlled thermal machines. While both a general theory of quantum feedback control as well as specific examples of quantum feedback-controlled engines have been presented, still lacking is a general framework for such machines. Here, we present a framework for a generic, two-stroke quantum heat engine interacting with N thermal baths and Maxwell's demon. The demon performs projective measurements on the engine working substance, the outcome of which is recorded in a classical memory, embedded in its own thermal bath. To perform feedback control, the demon enacts unitary operations on the working substance, conditioned on the recorded outcome. By accounting for the thermodynamic cost of measurement, and hence considering the machine-memory compound as a hybrid (quantum-classical) standard thermal machine interacting with $N+1$ thermal baths, our framework puts the working substance and memory on equal footing, thereby enabling a comprehensible resolution to Maxwell's paradox and elucidating the intricate manner in which information impacts the performance of quantum engines. We illustrate the application of our framework with a two-qubit engine. A remarkable observation is that more information does not necessarily result in better thermodynamic performance: sometimes knowing less is better.

DOI: 10.1103/t1wl-p415

I. INTRODUCTION

Quantum thermodynamics, which aims to elucidate the fundamental principles of thermodynamics in the quantum regime, has progressed rapidly over the last couple of decades [1–5]. Spurred in part by the miniaturization of technological devices, the development of quantum thermodynamics is crucial for improving design and performance of microscopic heat engines and refrigerators [6–15]. Of particular interest is the role that information plays in such systems, an avenue that is currently being explored within the framework of feedback-controlled thermal machines. Such machines harness information gained via measurement of the working substance (WS) to steer the evolution of the system, potentially providing performance enhancement or even enabling processes that would otherwise be forbidden [16–18].

Work along this theme began with the famous thought experiment of Maxwell's demon [19], an intelligent being that seemed able to violate the second law of thermodynamics by utilizing information to reduce entropy in a closed system. The concept of information as a quantifiable resource in thermodynamic processes was further elucidated with the introduction of Szilard's engine, an engine fueled by information [20]. Eventually, the demon was exorcised, restoring the second law of thermodynamics, by recognizing that writing and erasure of information in the demon's memory must be taken into account when calculating the total entropy change in the system [21,22]. There have been continued efforts to better understand the nature and role of information in thermodynamics processes in the quantum regime [23–31], while a number of experimental works have demonstrated the use of information in quantum thermal engines [32–38]. However, a complete understanding of the impact of information in thermal engines is still under active investigation (see Ref. [39] for a review, in particular Sec. VIII C).

While there are specific examples of feedback-controlled quantum heat engines in the literature, a general framework has yet to be presented. Meanwhile, the highly abstracted theory of quantum feedback control by Sagawa and Ueda [26] is so general that its application to quantum heat engines is not immediately apparent. In this paper, we aim to bridge this gap between explicit examples and general theory by grounding feedback-controlled quantum heat engines in a more physically tangible framework.

Specifically, we consider a multibath system, depicted schematically in Fig. 1, comprising a two-stroke heat engine, which undergoes measurement and feedback control, combined with a classical memory that stores the information collected from the measurement. The heat engine itself is composed of a bipartite (or in general, a multipartite) WS, in which each component can be independently coupled or decoupled to its own thermal bath at a distinct temperature. Likewise, the classical memory is also coupled to its own thermal bath. We highlight that an advantage of our framework is that it treats the WS and the demon's memory on equal footing, removing some of the often perceived mysteriousness of the demon's actions. This enables us to derive what we believe to be a particularly comprehensible and accessible

Published by the American Physical Society under the terms of the Creative Commons Attribution 4.0 International license. Further distribution of this work must maintain attribution to the author(s) and the published article's title, journal citation, and DOI.

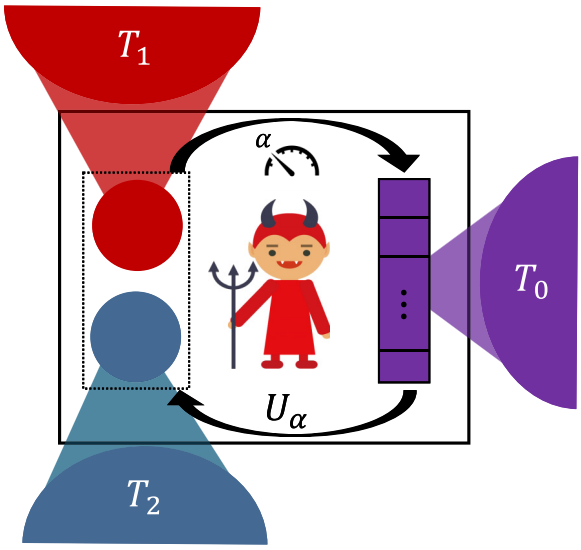


FIG. 1. Schematic of the physical model for a feedback-controlled quantum heat engine. The multipartite WS of the heat engine, outlined in a dotted black rectangle, is composed of quantum systems, each in contact with their own thermal bath, possibly at different temperatures, $T_1, \ldots, T_N$. The extended working substance, outlined by the solid black rectangle, extends the heat engine to include the demon's memory, which is in thermal contact with yet another thermal bath at temperature T_0. The demon measures the WS, writing the result α into memory. Based on the value of α, the demon enacts a corresponding unitary U_α on the WS.

exorcism of Maxwell's demon, thereby rigorously restoring the second law of thermodynamics within our model.

We next leverage our model to explore the efficiency of feedback-controlled quantum heat engines. The large number of free parameters in the system presents a Pandora's box of scenarios to study. However, we narrow our focus to a few relevant regimes of initial conditions and types of projective measurements to uncover several intriguing observations. In particular, we prove that for fine-grain measurements (which we define more formally later), there exists an optimal measurement basis that maximizes the engine's efficiency. In addition, and perhaps counterintuitively, we find that in some scenarios, coarse-grain measurements can lead to greater efficiency than fine-grain measurements; in other words, sometimes knowing less is better. Our findings provide valuable insights into the interplay of information and energy conversion at the quantum scale, offering guidance for the design of practical quantum thermal devices.

II. THEORY

A. The working substance

We consider a multipartite quantum system as the WS of the thermal machine. Let

$$H = \sum_{i=1}^{N} H_i \tag{1}$$

denote the WS Hamiltonian, with H_i the Hamiltonian of each partition thereof. For the sake of simplicity we restrict the discussion to the so-called two-stroke cycle [6,12]. In the two-stroke cycle, the WS begins in a multipartite Gibbs state ρ, featuring each partition at thermal equilibrium with possibly distinct temperatures, written as

$$\rho = \bigotimes_{i=1}^{N} \frac{e^{-\beta_i H_i}}{Z_i}, \quad Z_i = \mathrm{Tr} e^{-\beta_i H_i}. \tag{2}$$

B. The first stroke

The first stroke begins with the WS undergoing a projective measurement of some observable

$$A = \sum_{\alpha=1}^{K} a_\alpha \Pi_\alpha \tag{3}$$

where a_α denote its eigenvalues, and Π_α denote the corresponding eigenprojectors. We shall denote with g_α the rank of projector Π_α, that is the degeneracy of the eigenvalue a_α. Here, K is the number of distinct eigenvalues of A, which is bounded by the WS Hilbert-space dimension $d = \sum_{\alpha=1}^{K} g_\alpha$. As a consequence of the measurement, one outcome, say outcome α, is produced and recorded in a classical memory. According to the postulates of quantum mechanics, the state ρ collapses onto

$$\rho_\alpha = \frac{\Pi_\alpha \rho \Pi_\alpha}{q_\alpha} \tag{4}$$

where

$$q_\alpha = \mathrm{Tr}\, \Pi_\alpha \rho \Pi_\alpha \tag{5}$$

is the probability that the αth outcome is produced. Note that the effect of the measurement on the WS is fully specified by the set of measurement projectors

$$\mathbf{\Pi} = \{\Pi_1, \ldots, \Pi_K\}. \tag{6}$$

The eigenvalues a_α do not play any role, hence in the following they will not be mentioned any more.

The demon has a collection of K unitaries, $U_\alpha, \alpha = 1 \ldots K$, and feedback control consists of the demon enacting unitary U_α on the WS, conditioned on the outcome α being measured. The post-feedback-control WS state then reads

$$\rho'_\alpha = U_\alpha \rho_\alpha U_\alpha^\dagger. \tag{7}$$

With this operation, the first stroke is completed.

Two points are worth stressing. First, during the first stroke the WS does not interact with any thermal bath. Second, in order to enact the unitary U_α the demon has to implement a cyclic time-dependent perturbation $V_\alpha(t)$, such that the resulting WS Hamilton function $H_\alpha(t) = H + V_\alpha(t)$ induces the desired unitary U_α. That is, V_α must be such that $U_\alpha = T \exp[-i/\hbar \int_0^\tau ds H_\alpha(s)]$. Typically $V_\alpha(t)$ will contain interaction terms among the various parts of the WS. In the following we shall only focus on the unitaries U_α without entering the separate problem of designing the according V_α.

C. The second stroke

The second stroke consists of placing each partition of the WS in weak thermal contact with its associated thermal bath

so that it reaches a state of thermal equilibrium and leads the WS back to the initial state Eq. (2), thereby closing the cycle.

D. Apparent violation of the second law

In order to access the compliance of our engine model with the second law of thermodynamics, we must first compute the change in the expectation value of the energy of each partition i across the first stroke, reading

$$\langle \Delta E_i \rangle = \mathrm{Tr} H_i(\rho' - \rho) \tag{8}$$

where

$$\rho' = \sum_{\alpha=1}^{K} q_\alpha \rho'_\alpha = \sum_{\alpha=1}^{K} U_\alpha \Pi_\alpha \rho \Pi_\alpha U_\alpha^\dagger = \mathcal{M}[\rho] \tag{9}$$

is the non-post-selected WS state at the end of the first stroke. Note that we denote with $\mathcal{M}$ the linear transformation that maps ρ onto ρ'.

As shown in Ref. [40], due to the special initial condition in Eq. (2), the following inequality holds:

$$\sum_{i=1}^{N} \beta_i \langle \Delta E_i \rangle \geqslant \Delta \mathcal{H} = \mathcal{H}[\rho'] - \mathcal{H}[\rho] \tag{10}$$

where $\mathcal{H}$ denotes von Neumann information,

$$\mathcal{H}[\sigma] = -\mathrm{Tr}\sigma \ln \sigma. \tag{11}$$

Depending on how the unitaries U_α are selected, the von Neumann information may increase, decrease, or remain constant. For example, if one and the same unitary is enacted regardless of the outcomes (i.e., no feedback control), that is $U_\alpha = U \ \forall \ \alpha$, the resulting map $\mathcal{M}$ would be unital, thus resulting in an overall increase in von Neumann information [41]. Therefore, active feedback control is necessary for compressing the von Neumann information [40].

Assuming the system-bath interaction energy is so weak that it can be neglected, the negative energy change $\langle \Delta E_i \rangle$ in each partition of the WS across the first stroke equals the average heat Q_i ceded by thermal bath i to the WS during the second stroke:

$$Q_i = -\langle \Delta E_i \rangle. \tag{12}$$

Thus, during the second stroke, the energies $\langle \Delta E_i \rangle$ that the parts of the WS recieve via interaction with the work source and the other parts during the first stroke are distributed to the thermal baths.

Combining Eq. (12) with Eq. (10), we have

$$\sum_{i=1}^{N} \beta_i Q_i \leqslant -\Delta \mathcal{H}. \tag{13}$$

When $\mathcal{M}$ induces a compression of von Neumann information $\Delta \mathcal{H} < 0$, it is possible that the Clausius sum $\sum_{i=1}^{N} \beta_i Q_i$ takes a positive value. In this case, it would *appear* that the second law of thermodynamics has been violated in a way that is completely analogous to Maxwell's demon paradox, except here the WS is a quantum system.

E. Reconciling the second law, exorcism of Maxwell's demon

Resolving the paradox of the apparent violation of the second law of thermodynamics requires taking into account the thermodynamic cost of the demon's information gathering. As widely discussed in the literature (see, e.g., Ref. [42]), due to the Landauer principle [21], the average energy, $\langle W \rangle_{\mathrm{m}}$, spent by the demon to gather information, i.e., to imprint the outcome labels α in the classical memory, obeys the bound

$$\langle W \rangle_{\mathrm{m}} \geqslant \beta_0^{-1} h[\{q_\alpha\}] \tag{14}$$

where

$$h[\{q_\alpha\}] \doteq -\sum_{\alpha=1}^{K} q_\alpha \ln q_\alpha \tag{15}$$

is the Shannon information of the distribution $\{q_\alpha\}$, where q_α is defined in Eq. (5), and β_0 is the inverse thermal energy of the bath in which the classical memory is embedded.

We stress that such an encoding process is nothing but the quantum measurement itself. In fact, a quantum measurement process is the process of imprinting information about the state of a quantum system into a large classical system (i.e., the classical memory), such that it can be read by a classical being (i.e., the demon). Accordingly, $\langle W \rangle_{\mathrm{m}}$ can be understood as the energetic cost of the quantum measurement.

It is important to clarify that with "imprinting information" in the memory, we mean setting the memory to the specific state α (corresponding to the state of the measured quantum system). Physically, such a process of "RESET to α" is equivalent to what Landauer calls an "erasure," so its minimal energetic cost is, in fact, given by Eq. (14), which is universally known as the cost of erasure, rather than "imprinting" [21]. Unfortunately, this nomenclature can raise some confusion, and we hope to have clarified the fact that erasure and imprinting are just two sides of the same coin. It is also worth remarking that, in our model, the memory need not be reset to any special state after imprinting the label α, because the next measurement will encode the new state α' regardless of the memory previous state α, which is the defining feature of the "RESET to" process [21,43].

A crucial result is the following inequality:

$$h[\{q_\alpha\}] \geqslant -\Delta \mathcal{H}, \tag{16}$$

which implies that the negative von Neumann information change in the WS is smaller than the Shannon information of the measurement outcomes.

A proof of Eq. (16) can be found in the Appendix, while here we discuss its most crucial consequence. Using Eq. (14), we get

$$\langle W \rangle_{\mathrm{m}} \geqslant -\beta_0^{-1} \Delta \mathcal{H} \tag{17}$$

which, when combined with Eq. (10), leads to the salient result

$$\beta_0 \langle W \rangle_{\mathrm{m}} + \sum_{i=1}^{N} \beta_i \langle \Delta E_i \rangle \geqslant 0 \tag{18}$$

or, equivalently,

$$\sum_{i=0}^{N} \beta_i Q_i \leqslant 0 \tag{19}$$

where we introduce the notation

$$Q_0 = -\langle W \rangle_{\mathrm{m}} \tag{20}$$

to denote the average heat ceded by the thermal bath coupled to the memory. Note that the sum in Eq. (19) runs from $i = 0$, and hence it includes the heat Q_0.

Equation (19) expresses the validity of the Clausius inequality (i.e., the second law of thermodynamics) for the hybrid (classical-quantum) extended WS (xWS) comprising the N-partite quantum WS and the classical memory. This crucial inequality allows us to treat the extended hybrid engine as a standard feedbackless heat engine comprising $N + 1$ thermal baths. Heat is exchanged between the WS and the thermal baths, while work is exchanged between an external agent that writes measurement outcomes into a classical memory (in contact with one of the thermal baths) and enacts the K unitaries U_α on the WS (in contact with the remaining N thermal baths).

Since, at the end of the two-stroke thermodynamic cycle, the WS returns to its initial state, assuming all memory states have the same energy, the total work output equals the total energy ceded by the baths. Thus, Eq. (19) is complemented by the following equation:

$$W_{\mathrm{out}} = \sum_{i=0}^{N} Q_i, \tag{21}$$

which expresses the first law of thermodynamics for the xWS. Here, W_{out} denotes the total work output of the xWS, which can be rewritten as

$$W_{\mathrm{out}} = \langle W \rangle_{\mathrm{fc}}^{\mathrm{out}} - \langle W \rangle_{\mathrm{m}}. \tag{22}$$

where $\langle W \rangle_{\mathrm{fc}}^{\mathrm{out}}$ is the work extracted from the WS across the first stroke by enacting the feedback control unitaries U_α, namely,

$$\langle W \rangle_{\mathrm{fc}}^{\mathrm{out}} = -\sum_{i=1}^{N} \langle \Delta E_i \rangle = \mathrm{Tr} H(\rho - \rho'). \tag{23}$$

Note that the W_{out} is the difference of two competing terms. The quantity $\langle W \rangle_{\mathrm{fc}}^{\mathrm{out}}$ is the energy output from the WS during the first stroke. The quantity $\langle W \rangle_{\mathrm{m}}$ is the energy input to perform measurements. We stress that the cost of measurement $\langle W \rangle_{\mathrm{m}}$ depends on measurement projectors $\boldsymbol{\Pi} = (\Pi_1, \ldots, \Pi_K)$ but not on the according unitaries $\boldsymbol{U} = (U_1, \ldots, U_K)$. In contrast, given the projectors $\boldsymbol{\Pi}$, the energy the demon gets out of the WS, $\langle W \rangle_{\mathrm{fc}}^{\mathrm{out}}$, depends on its choice of the unitaries $\boldsymbol{U}$.

As will be discussed in more detail below, in Sec. V and illustrated with the examples in Sec. VI, this gives rise to a highly complex tradeoff between the utility of the information and the cost to retrieve it.

Note that in the case of a single heat bath (that thermalizes both the WS and memory), Eq. (19) boils down to

$$W_{\mathrm{out}} \leqslant 0 \tag{24}$$

expressing the Kelvin postulate of the second law: no energy can be extracted from a single thermal bath by the application of a cyclical driving. This generalizes the classical result of Ref. [42] to the quantum case.

III. EFFICIENCY OF HEAT ENGINES

Depending on the relative signs of W_{out} and Q_i, distinct operation modes of the engine can be realized [44,45]. The most relevant are the "heat engine" mode, characterized by positive work output, and the "refrigeration mode," characterized by positive heat extraction from the lowest-temperature bath. In the following, we shall focus on the heat engine operation, i.e., we shall assume $W_{\mathrm{out}} > 0$, which in turn implies that we are considering the case in which there are at least two distinct temperatures T_i.

In this regime the thermodynamic efficiency is given by

$$\eta = \frac{W_{\mathrm{out}}}{Q_{\mathrm{in}}} \tag{25}$$

where Q_{in} is the total heat intake per cycle:

$$Q_{\mathrm{in}} = \sum_{i=0}^{N} [Q_i]_+ \tag{26}$$

where $[x]_+ = x\theta(x)$ with θ denoting the Heaviside step function. In other words, Q_{in} is given by the sum of all positive values Q_i.

According to Ref. [46], Eqs. (19) and (21) imply that η is bounded by the Carnot efficiency η^C [47]:

$$\eta \leqslant 1 - \frac{T_{\mathrm{min}}}{T_{\mathrm{max}}} \doteq \eta^C \tag{27}$$

where η^C is expressed in terms of the largest temperature T_{max} of all the baths that give away heat, and the smallest temperature T_{min} of all the baths that receive heat [48],

$$T_{\mathrm{min}} = \min_{\{i|Q_i<0\}} \beta_i^{-1}, \quad T_{\mathrm{max}} = \max_{\{i|Q_i>0\}} \beta_i^{-1}. \tag{28}$$

In the context of our xWS, Q_{in} is the sum of the individual heat intakes of each of the $N + 1$ thermal baths, Eq. (26). Recall that index $i = 0$ denotes the memory bath, while $i = 1 \ldots N$ denote the thermal baths associated with the WS. In general, according to Eqs. (14) and (20) the heat ceded by the memory bath

$$Q_0 \leqslant -\beta_0^{-1} h[\{q_\alpha\}] \leqslant 0 \tag{29}$$

because the Shannon information is non-negative. This inequality reflects the fact that in the present setup, the memory bath always receives a positive heat since the process of memory imprinting is dissipative. Thus, the total heat intake can be rewritten

$$Q_{\mathrm{in}} = \sum_{i=1}^{N} [Q_i]_+ \tag{30}$$

where the sum now runs from $i = 1$.

Using Eq. (21), we have

$$\eta = \frac{\sum_{i=1}^{N} Q_i}{Q_{\mathrm{in}}} + \frac{Q_0}{Q_{\mathrm{in}}}. \tag{31}$$

In general, Q_0 will depend on the intricacies of how the demon performs its information gathering. However, the Landauer bound Eq. (14) sets a maximum for its value as

$$Q_0^L = -T_0 h[\{q_\alpha\}] \tag{32}$$

where $T_0 = \beta_0^{-1}$ is the temperature of the memory bath. Therefore, in the following, we shall focus on what we will call the "Landauer efficiency"

$$\eta^L = \frac{\sum_{i=1}^N Q_i}{Q_{\text{in}}} - \frac{h[\{q_\alpha\}]}{Q_{\text{in}}} T_0 \tag{33}$$

which denotes the efficiency achieved when the Landauer bound is saturated, i.e., when Q_0 takes on its maximal value. We emphasize, however, that in any realistic realization of the engine, the actual efficiency η will be smaller than η^L,which in turn is smaller than Carnot efficiency η^C:

$$\eta \leqslant \eta^L \leqslant \eta^C. \tag{34}$$

Note that the cost of information gathering only enters η^L linearly through T_0. The smaller T_0 the higher η^L, reflecting that less dissipation is incurred gathering in information at lower memory bath temperature.

IV. MAXIMUM LANDAUER EFFICIENCY

It is interesting to analyze the maximum Landauer efficiency that can be achieved in feedback-controlled quantum heat engines. For fixed WS Hamiltonian H and bath temperatures, $\boldsymbol{\beta} = (\beta_0, \beta_1, \ldots, \beta_N)$, the Landauer efficiency η^L depends on the measurement projectors $\boldsymbol{\Pi} = (\Pi_1, \ldots, \Pi_K)$ and the associated feedback unitaries $\boldsymbol{U} = (U_1, \ldots, U_K)$. In particular, for a given set of measurement projectors $\boldsymbol{\Pi}$, η^L changes depending on the choice of unitaries $\boldsymbol{U}$. In the following, we shall use the notation $\bar{\eta}^L$ to denote the maximum of η^L over all possible choices of feedback unitaries $\boldsymbol{U}$. That is (leaving the dependence on H, $\boldsymbol{\beta}$ implicit, in order to keep the notation light),

$$\bar{\eta}^L(\boldsymbol{\Pi}) \doteq \max_{\boldsymbol{U}} \eta^L(\boldsymbol{\Pi}, \boldsymbol{U}). \tag{35}$$

For simplicity, we shall call it the "max Landauer efficiency."

In order to analyze the max Landauer efficiency, it is helpful to distinguish between two main paradigms of measurement: fine-grain and coarse-grain measurement. Fine-grain measurement refers to measurements in which the rank of all the measurement projectors Π_α is unity. A coarse-grained measurement refers to any measurement in which at least one projector has rank larger than 1.

A. Fine-grain measurement

It is convenient to introduce the spectral decomposition of the Hamiltonian

$$H = \sum_{k=1}^{d} e_k \left|e_k\right\rangle \left\langle e_k\right| \tag{36}$$

in terms of its ordered eigenvalues $e_1 \leqslant e_2 \cdots \leqslant e_d$ and eigenvectors $|e_k\rangle$. We shall use the symbol

$$\boldsymbol{E} = \left(\left|e_1\right\rangle \left\langle e_1\right|, \ldots, \left|e_d\right\rangle \left\langle e_d\right|\right) \tag{37}$$

to denote the complete set of fine-grain measurement operators of H.

A first remarkable result is the following: given a generic set of fine-grain measurement operators, $\boldsymbol{F} = \left(\left|f_1\right\rangle \left\langle f_1\right|, \ldots, \left|f_d\right\rangle \left\langle f_d\right|\right)$, where $\left(\left|f_1\right\rangle, \ldots, \left|f_d\right\rangle\right)$ form a complete orthonormal basis of the WS Hilbert space, we have

$$\bar{\eta}^L(\mathbf{F}) = 1 - \frac{h[\{q_k\}]}{\bar{Q}_{\text{in}}} T_0 \tag{38}$$

where $q_k = \left\langle f_k\right| \rho \left|f_k\right\rangle$ is the probability that the k^{th} outcome of the measurement is produced, and

$$\bar{Q}_{\text{in}} = \text{Tr} H(\rho - \left|e_1\right\rangle \left\langle e_1\right|) \tag{39}$$

is the difference between the WS ground-state energy and its initial energy.

To prove Eq. (38), note that η^L, Eq. (33), is composed of two terms. The first term $\sum_{i=1}^N Q_i / \sum_{i=1}^N [Q_i]_+$ is smaller than or equal to 1, due to the inequality $x \leqslant [x]_+$. Its maximum value, i.e., 1, is obtained when all Q_i's (with $i > 0$) are positive. The second term $h[\{q_k\}]/Q_{\text{in}}$ is minimized when Q_{in} is maximum (note that the numerator does not depend on the unitaries U_k). Such maximum occurs when the unitaries U_k are the unitaries $\bar{U}_k$ that extract the highest amount of energy (i.e., the ergotropy [49]) from the postselected states ρ_k. We refer to these unitaries as *ergotropy unitaries*, which in general send the postselected states ρ_k to their passive companion states $\breve{\rho}_k$.

Since the postmeasurement states $\rho_k = \left|f_k\right\rangle \left\langle f_k\right|$ of fine-grain measurement are pure, their passive companion is the ground state $\left|e_1\right\rangle \left\langle e_1\right|$ for all k's and the ergotropy unitaries for fine-grain measurement satisfy

$$\bar{U}_k \left|f_k\right\rangle = e^{-i\phi_k} \left|e_1\right\rangle, \quad k = 1 \ldots d. \tag{40}$$

Thus, when such unitaries $\bar{U}_k$ are chosen for feedback control, the post-feedback-control state, Eq. (9), is the WS Hamiltonian ground state, $\rho' = \left|e_1\right\rangle \left\langle e_1\right|$. Given that the WS Hamiltonian is the direct sum of the N local Hamiltonians H_i, the ground state is the tensor product of the ground states of each partition. Thus, the unitaries $\bar{U}_k$ individually maximize each term Q_i (with $i > 0$). Since all such maximum Q_i's are trivially non-negative, their sum amounts to Q_{in}, Eq. (30), which thus attains its maximal value $\bar{Q}_{\text{in}}$ in Eq. (39).

Note that this value is 1 and the same regardless of the set of measurement projectors, as long as they are all rank 1. Furthermore, the positivity of all Q_i's (with $i > 0$) also ensures maximization of the first term $\sum_{i=1}^N Q_i / \sum_{i=1}^N [Q_i]_+$, which attains unit value. Accordingly, the difference of the two terms in Eq. (33), i.e., the Landauer efficiency η^L, is maximized by the ergotropy unitaries, Eq. (40), and amounts to the value in Eq. (38).

A remarkable aftermath of Eq. (38) is that, among all fine-grain measurement sets, the largest value of the max Landauer efficiency is achieved when measuring in the WS Hamiltonian eigenbasis $\boldsymbol{E}$. That is,

$$\max_{\boldsymbol{F}} \bar{\eta}^L(\boldsymbol{F}) = \bar{\eta}^L(\boldsymbol{E}). \tag{41}$$

To prove Eq. (41) note that the measurement operators enter Eq. (38) only through the Shannon information. Thus, we only need to show that the Shannon information $h[\{\cdot\}]$ is

minimal among all fine-grain measurements when measuring over the set $\boldsymbol{E}$. Let

$$\rho = \sum_{n=1}^{d} p_n \left|e_n\right\rangle \left\langle e_n\right| \tag{42}$$

be the spectral decomposition of the initial state [recall that, by construction, ρ, Eq. (2), is diagonal in the WS Hamiltonian eigenbasis]. Using Eq. (42), we get

$$q_k = \left\langle f_k\right| \rho \left|f_k\right\rangle = \sum_{n=1}^{d} p_n \left\langle f_k|e_n\right\rangle \left\langle e_n|f_k\right\rangle . \tag{43}$$

Note that $P_{kn} \doteq \left\langle f_k|e_n\right\rangle \left\langle e_n|f_k\right\rangle = \left|\left\langle f_k|e_n\right\rangle\right|^2$ are the elements of a bistochastic matrix, therefore [50]

$$h[\{q_k\}] = h\left[\left\{\sum_n P_{kn} p_n\right\}\right] \geqslant h[\{p_k\}]. \tag{44}$$

Thus, the fine-grain measurement over the Hamiltonian eigenbasis $\boldsymbol{E}$ is the one that collects the smallest amount of information, hence dissipates the least amount of heat in the memory bath, and thus achieves the largest max Landauer efficiency.

B. Coarse-grain measurement

The picture gets considerably more complicated when coarse-grain measurements are considered. As will become clear with the illustrative examples below, in this case the ergotropy unitaries $\bar{U}_\alpha, \alpha = 1 \ldots K < d$ do not all send the state of the system to one and the same state ρ'_α as in the case of fine-grain measurement, nor do they generally extract energy from all baths $i = 1 \ldots N$. Thus, Eq. (38) does not apply in this case, nor does it appear plausible that a similar simple analytical formula can be found. Depending on the specific setup, it can be difficult to find the set of unitaries that maximize η^L due to its nonlinearity, and the problem should be generally treated numerically.

It is important to remark that using coarse-grain measurements is a way to collect less information, thereby dissipating less heat into the memory bath and increasing efficiency. Less information, however, can negatively impact heat extraction from the other baths, thereby reducing work output and decreasing efficiency. Thus, there is a tradeoff between the cost of gathering information and the gain one can derive from it. As we shall see in the examples below, sometimes knowing less can be advantageous.

V. LANDAUER EFFICIENCY AT MAXIMUM WORK OUTPUT

Depending on the application, it may be more desireable to maximize work output, rather than the efficiency when designing a heat engine. Therefore, we now turn our attention to the Landauer efficiency at maximum work output, which we denote by $\eta_W^L(\boldsymbol{\Pi})$, and call it the "max-work Landauer efficiency." It is similar to the "efficiency at maximum power" of Curzon and Ahlborn [51]. It is defined as the value that the Landauer efficiency $\eta^L(\boldsymbol{\Pi}, \boldsymbol{U})$, Eq. (33), attains when the unitaries $\boldsymbol{U}$ are chosen to maximize the work output.

Note that the unitaries only enter W_{out}, Eq. (22), through the term $\langle W\rangle_{\text{fc}}^{\text{out}}$. Thus, maximizing W_{out} is equivalent to maximizing $\langle W\rangle_{\text{fc}}^{\text{out}} = \sum_{i=1}^{N} Q_i = \text{Tr}H(\rho - \rho')$, Eqs. (23) and (12). The ergotropy unitaries $\bar{U}_\alpha$ send each postselected state ρ_α to its passive companion $\rho'_\alpha = \breve{\rho}_\alpha = \bar{U}_\alpha \rho_\alpha \bar{U}_\alpha^\dagger$, featuring the smallest possible total energy $\text{Tr}H\breve{\rho}_\alpha$. Thus, their convex combination

$$\breve{\rho} = \sum_\alpha q_\alpha \breve{\rho}_\alpha \tag{45}$$

features the smallest total energy among all possible non-postselected states ρ'. Therefore we have

$$\eta_W^L(\boldsymbol{\Pi}) = \eta^L(\boldsymbol{\Pi}, \bar{\boldsymbol{U}}) \tag{46}$$

which holds regardless of the grain of the measurement.

By setting the cost of information gathering to its minimal Landauer value, Eq. (32), the maximum total work output achievable is given by

$$W_{\text{out}}^{\max} = \text{Tr}H(\rho - \breve{\rho}) - h[\{q_\alpha\}]T_0. \tag{47}$$

For fine-grain measurements, the ergotropy unitaries $\bar{\boldsymbol{U}}$ maximize both the Landauer efficiency and the total work output, that is,

$$\eta_W^L(\boldsymbol{F}) = \bar{\eta}^L(\boldsymbol{F}) \tag{48}$$

where $\boldsymbol{F}$ represents any set of fine-grain measurement projectors. In this case, the minimal energy state $\breve{\rho}$ is nothing but the ground state, and the maximum total work output is given by

$$W_{\text{out}}^{\max} = \text{Tr}H(\rho - \left|e_1\right\rangle \left\langle e_1\right|) - h[\{q_k\}]T_0. \tag{49}$$

In general, $\breve{\rho}$ depends on the operators $\boldsymbol{\Pi}$, but takes one and the same value $\left|e_1\right\rangle \left\langle e_1\right|$ for all fine-grain measurements. As anticipated above, compared to fine-grain measurement, a coarse-grain measurement would exhibit a smaller value of WS output work $\text{Tr}H(\rho - \breve{\rho})$. This, however, is paired with a smaller value of information gathering cost $h[\{q_k\}]T_0$, which gives rise to an intricate cost-benefit tradeoff.

VI. ILLUSTRATIVE EXAMPLES

We now apply our framework to an explicit physical model to analyze the max-work Landauer efficiency η_W^L of feedback-controlled quantum heat engines. Specifically, we consider a WS composed of two two-level systems (e.g., qubits). The WS Hamiltonian Eq. (1) is given by

$$H = \frac{\hbar\omega_1}{2}\sigma_1^z + \frac{\hbar\omega_2}{2}\sigma_2^z \tag{50}$$

with ω_i the resonant frequency of qubit i and σ_i^z the Pauli-Z operator on qubit i. Furthermore, each qubit is weakly connected to its own thermal bath at temperature $T_i = 1/\beta_i$ during the second stroke.

Let the energy eigenstates of qubit i be written as $\left|0\right\rangle_i$ and $\left|1\right\rangle_i$, which denote the ground and excited states, respectively. The eigenstates of the two-qubit WS can thus be written as $\left|a\right\rangle_1 \otimes \left|b\right\rangle_2 = \left|ab\right\rangle$, with $a, b \in \{0, 1\}$. In the following, all explicit matrices will be written in the computational basis, which coincides with the energy eigenbasis of the system, $\{\left|00\right\rangle, \left|01\right\rangle, \left|10\right\rangle, \left|11\right\rangle\}$.

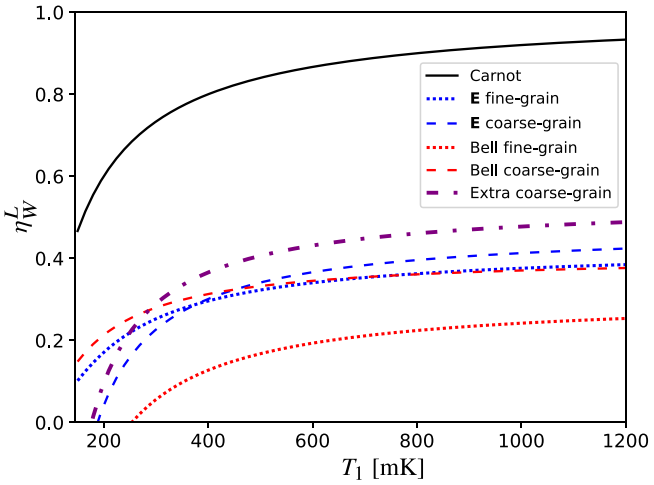


FIG. 2. Comparison of max-work Landauer efficiency η_W^L for fine- and coarse-grain measurement in the $\boldsymbol{E}$ and Bell bases as a function of bath temperature T_1 of qubit 1.

In the following subsections, we consider using this WS in a feedback-controlled two-stroke quantum heat engine. We examine the max-work Landauer efficiency η_W^L as a function of the bath temperature T_1 of qubit 1 in Fig. 2. We compare efficiencies for various sets of projective measurements with the blue, red, and purple curves and include for reference the Carnot efficiency with the solid black curve. We plot the maximal work extracted from the WS $\langle W\rangle_{\rm fc}^{\rm out} = {\rm Tr}H(\rho - \breve{\rho})$, the minimal cost of information gathering $\langle W\rangle_{\rm m} = -Q_0^L = h[\{q_k\}]T_0$, and the maximal total work output $W_{\rm out}$, Eq. (47), in Fig. 3, which give insights into the crossing of curves observed in Fig. 2. For all plots, we use the following fixed parameters: the temperature of the bath connected to qubit 2 $T_2 = 150$ mK, the temperature of the memory bath $T_0 = 80$ mK, and the frequency of both qubits $\omega_i/2\pi = f = 5$ GHz.

A. Fine-grain measurement in the E basis

We first consider fine-grain measurement of the WS Hamiltonian H, defined by the set of projectors in Eq. (37) denoted by $\boldsymbol{E}$. In this case, the four projectors are defined as

$$E_{00} = |00\rangle\langle 00|, \quad E_{01} = |01\rangle\langle 01|, \quad E_{10} = |10\rangle\langle 10|, \quad E_{11} = |11\rangle\langle 11|. \tag{51}$$

Measurement will collapse the state of the system into one of the states $\rho_\alpha = |\alpha\rangle\langle\alpha|$, $\alpha \in \{00, 01, 10, 11\}$ with probability $q_\alpha = \langle\alpha|\rho|\alpha\rangle$. Explicitly,

$$q_{00} = \frac{e^{\frac{\beta_1\hbar\omega_1}{2}}}{Z_1}\frac{e^{\frac{\beta_2\hbar\omega_2}{2}}}{Z_2}, \quad q_{01} = \frac{e^{\frac{\beta_1\hbar\omega_1}{2}}}{Z_1}\frac{e^{\frac{-\beta_2\hbar\omega_2}{2}}}{Z_2},$$
$$q_{10} = \frac{e^{\frac{-\beta_1\hbar\omega_1}{2}}}{Z_1}\frac{e^{\frac{\beta_2\hbar\omega_2}{2}}}{Z_2}, \quad q_{11} = \frac{e^{\frac{-\beta_1\hbar\omega_1}{2}}}{Z_1}\frac{e^{\frac{-\beta_2\hbar\omega_2}{2}}}{Z_2} \tag{52}$$

where $Z_i = {\rm Tr}e^{-\beta_i H_i} = 2\cosh(\beta_1\hbar\omega_i/2)$ is the partition function of the $i^{\rm th}$ partition of the WS. Feedback control consists of applying an associated unitary U_α based on the outcome of the measurement. To achieve maximum total work output, we select a set of ergotropy unitaries, as defined in Eq. (40). Explicitly, we define the feedback unitaries to be

$$U_{00} = \begin{pmatrix}1&0&0&0\\0&1&0&0\\0&0&1&0\\0&0&0&1\end{pmatrix}, \quad U_{01} = \begin{pmatrix}0&1&0&0\\1&0&0&0\\0&0&1&0\\0&0&0&1\end{pmatrix},$$
$$U_{10} = \begin{pmatrix}0&0&1&0\\0&1&0&0\\1&0&0&0\\0&0&0&1\end{pmatrix}, \quad U_{11} = \begin{pmatrix}0&0&0&1\\0&1&0&0\\0&0&1&0\\1&0&0&0\end{pmatrix}. \tag{53}$$

Note that each U_α is simply a permutation between the energy eigenstate $|\alpha\rangle$ and the ground state (i.e., the lowest-energy eigenstate).

The final state after measurement and application of the associated feedback unitary is $\rho'_\alpha = U_\alpha\rho_\alpha U_\alpha^\dagger = |00\rangle\ \forall\,\alpha$. The non-post-selected final state is $\rho' = \sum_\alpha q_\alpha|00\rangle = |00\rangle$. The average change in energy of each qubit i can thus be computed with Eq. (8), plugging in the ground state for ρ'. Since ρ' is the ground state, we will have $\langle\Delta E_i\rangle \leqslant 0$ for both qubits, and thus $Q_i \geqslant 0$ for both qubits, according to Eq. (12). Therefore, $Q_{in} = \sum_{i=1}^2 Q_i = -\sum_{i=1}^2\langle\Delta E_i\rangle$.

The max-work Landauer efficiency η_W^L for fine-grain measurement in the $\boldsymbol{E}$ basis is shown by the dotted blue curve in Fig. 2. Likewise, the dotted blue curves in Fig. 3 plot the average extracted work [Fig. 3(a)], the cost of information gathering [Fig. 3(b)], and the total work output [Fig. 3(c)] for this measurement. These will be compared with various other projective measurements in the following subsections.

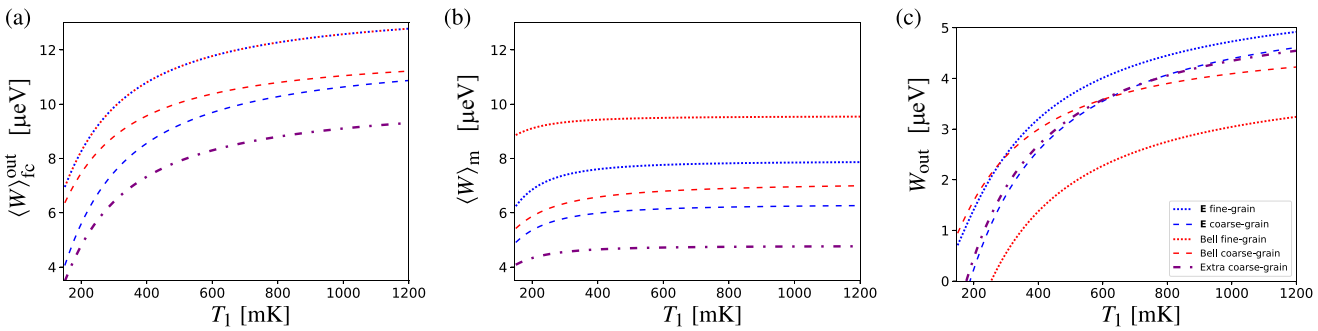


FIG. 3. Comparison of (a) feedback control work extraction, $\langle W\rangle_{\rm fc}^{\rm out}$, (b) Landauer cost of information gathering $\langle W\rangle_{\rm m}$, and (c) total work output $W_{\rm out}$, for fine- and coarse-grain measurements in the $\boldsymbol{E}$ and Bell bases as a function of bath temperature T_1 of qubit 1.

B. Coarse-grain measurement in the *E* basis

We next consider a coarse-grain measurement in the $\boldsymbol{E}$ basis. There are an infinite number of ways to perform a coarse-grained measurement, but we select an intuitive one here for explicit illustration.

We define the coarse-grain measurement projectors as

$$\Pi_1 = E_{00}, \quad \Pi_2 = E_{01} + E_{10}, \quad \Pi_3 = E_{11}. \tag{54}$$

In words, this measures how many excitations are present in the system (either 0, 1, or 2). Measurement will produce the states

$$\rho_1^C = \begin{pmatrix} 1 & 0 & 0 & 0 \\ 0 & 0 & 0 & 0 \\ 0 & 0 & 0 & 0 \\ 0 & 0 & 0 & 0 \end{pmatrix},$$
$$\rho_2^C = \frac{1}{q_{01}+q_{10}} \begin{pmatrix} 0 & 0 & 0 & 0 \\ 0 & q_{01} & 0 & 0 \\ 0 & 0 & q_{10} & 0 \\ 0 & 0 & 0 & 0 \end{pmatrix},$$
$$\rho_3^C = \begin{pmatrix} 0 & 0 & 0 & 0 \\ 0 & 0 & 0 & 0 \\ 0 & 0 & 0 & 0 \\ 0 & 0 & 0 & 1 \end{pmatrix} \tag{55}$$

with associated probabilities $p_1 = q_{00}$, $p_2 = q_{01} + q_{10}$, and $p_3 = q_{11}$, respectively, where the q_α are defined in Eq. (52).

Again, we select a set of ergotropy unitaries to maximize total work output. Following Ref. [49], these can be constructed as unitaries which sort the eigenvalues of the corresponding postmeasurement density matrix of the WS in nonincreasing order. We define unitaries $U_1 = U_{00}$ and $U_3 = U_{11}$ as previously defined in the fine-grain case. The feedback unitary U_2^C associated to Π_2 is written explicitly as

$$U_2^C = \begin{cases} \begin{pmatrix} 0 & 0 & 1 & 0 \\ 0 & 1 & 0 & 0 \\ 1 & 0 & 0 & 0 \\ 0 & 0 & 0 & 1 \end{pmatrix} & \text{if } q_{10} > q_{01} \\ \begin{pmatrix} 0 & 1 & 0 & 0 \\ 0 & 0 & 1 & 0 \\ 1 & 0 & 0 & 0 \\ 0 & 0 & 0 & 1 \end{pmatrix} & \text{if } q_{01} > q_{10}. \end{cases} \tag{56}$$

Since the q_α are determined by the initial parameters of the WS, we know at the outset of the problem how to define U_2^C. Note that in the case of coarse-grain measurement, the final state after measurement and feedback ρ' will not always be the pure ground state, but rather a mixture of states, which reduces the work extracted from the WS and, thus, the total work output.

The max-work Landauer efficiency η_W^L when using this coarse-grain measurement is plotted by the dashed blue curve in Fig. 2. We compare this with fine-grain measurement in the same basis (dotted blue curve), which shows there is a crossover point in efficiency. This highlights the intriguing observation that more information is not always better. Indeed, there is a real cost to gathering information from a system, and given a particular set of initial parameters, it may be more efficient to gather less information.

Figure 3 provides some insight into the crossover in max-work Landauer efficiencies between the fine- and coarse-grain measurements. Figure 3(c) shows that the total work output is only slightly greater in the fine-grain case (dotted blue curve) versus the coarse-grain case (dashed blue curve) for measurement in the $\boldsymbol{E}$ basis. However, there is a larger gap between the two cases for the cost of gathering information, Fig. 3(b). While the efficiency in the fine-grain case is augmented with greater work output, it is hampered by the larger cost of gathering information. Thus, when the cost of information gathering is not well compensated by its corresponding improvement in work output, coarse-grained measurements may have an advantage over fine-grained measurement in terms of efficiency.

C. Fine-grain measurement in the Bell basis

We next turn to performing measurements in the Bell basis, given by

$$|\Phi^\pm\rangle = \frac{1}{\sqrt{2}}(|00\rangle \pm |11\rangle), \quad |\Psi^\pm\rangle = \frac{1}{\sqrt{2}}(|01\rangle \pm |10\rangle). \tag{57}$$

We consider a fine-grain measurement in this basis defined by the four projectors

$$\Pi_1^B = |\Phi^+\rangle\langle\Phi^+|\, \Pi_2^B = |\Psi^+\rangle\langle\Psi^+|,$$
$$\Pi_3^B = |\Phi^-\rangle\langle\Phi^-|\, \Pi_4^B = |\Psi^-\rangle\langle\Psi^-|. \tag{58}$$

Measurement will collapse the state of the system into one of the Bell states Π_α^B with probability $p_\alpha^B = \mathrm{Tr}\rho\Pi_\alpha^B$. Explicitly, $p_1^B = p_3^B = \frac{1}{2}(q_{00} + q_{11})$ and $p_2^B = p_4^B = \frac{1}{2}(q_{01} + q_{10})$, where the q_α were defined in Eq. (52).

One way to determine the ergotropy unitaries for maximal total work output is as follows. First, define a unitary transformation U_t that rotates each Bell state to a unique eigenstate of the Hamiltonian H. Applying U_t to the measured Bell state will transform the state to its corresponding eigenstate of H. Next, the appropriate unitary U_α from Eq. (53) can be applied to transform the state to the ground state of the system. Thus, the feedback unitary for each outcome of the fine-grain Bell-basis measurement can be derived by composing U_t with the associated U_α.

Explicitly, we define U_t as

$$U_t = \frac{1}{\sqrt{2}} \begin{pmatrix} 1 & 0 & 0 & 1 \\ 0 & 1 & 1 & 0 \\ 1 & 0 & 0 & -1 \\ 0 & 1 & -1 & 0 \end{pmatrix} \tag{59}$$

which leads to the following feedback unitaries for maximal work output:

$$U_1^B = U_t U_{00}, \quad U_2^B = U_t U_{01},$$
$$U_3^B = U_t U_{10}, \quad U_4^B = U_t U_{11}. \tag{60}$$

All feedback unitaries U_i^B map the postmeasurement state to the pure ground state. Thus, as in the case for fine-grain measurement in the $\boldsymbol{E}$ basis, the final state after measurement and feedback is $\rho'_\alpha = |00\rangle\langle 00|\ \forall\, \alpha$.

The max-work Landauer efficiency η_W^L for fine-grain measurement in the Bell basis is shown by the dotted red curve in Fig. 2. As expected for fine-grain measurements, η_W^L is strictly smaller in the Bell basis (or in any other basis) than in the $\boldsymbol{E}$ basis, since we showed that the $\boldsymbol{E}$ basis has optimal efficiency in the fine-grain measurement setting. Figure 3(c) shows that total work output for fine-grain Bell measurement is the lowest of all measurements considered, while Fig. 3(b) shows that the cost of information gathering is the highest. These both negatively impact the efficiency, explaining why coarse-grain measurement in the Bell basis leads to the lowest efficiency of all measurements considered, as shown in Fig. 2.

D. Coarse-grain measurement in the Bell basis

We next turn to coarse-grained measurement in the Bell basis. We select a coarse-graining that is analogous to the coarse-grain measurement in the $\boldsymbol{E}$ basis (i.e., two rank-1 projectors and one rank-2 projector), defined by the following set of projectors:

$$\Pi_1^{CB} = \Pi_2^B, \quad \Pi_2^{CB} = \Pi_4^B, \quad \Pi_3^{CB} = \Pi_1^B + \Pi_3^B. \tag{61}$$

Measurement will collapse the state of the system into the states

$$\rho_1^{CB} = \Pi_2^B, \quad \rho_2^{CB} = \Pi_4^B,$$
$$\rho_3^{CB} = \frac{1}{q_{00}+q_{11}} \begin{pmatrix} q_{00} & 0 & 0 & 0 \\ 0 & 0 & 0 & 0 \\ 0 & 0 & 0 & 0 \\ 0 & 0 & 0 & q_{11} \end{pmatrix} \tag{62}$$

where the q_α are defined in Eq. (52), with associated probabilities $p_1^{CB} = p_2^B$, $p_2^{CB} = p_4^B$, and $p_3^{CB} = p_1^B + p_3^B$, with p_i^B defined in Sec. VI C. We again select ergotropy unitaries to maximize total work output, written explicitly as

$$U_1^{CB} = U_2^B, \quad U_2^{CB} = U_4^B, \quad U_3^{CB} = \begin{pmatrix} 1 & 0 & 0 & 0 \\ 0 & 0 & 0 & 1 \\ 0 & 0 & 1 & 0 \\ 0 & 1 & 0 & 0 \end{pmatrix} \tag{63}$$

where U_i^B were defined in Eq. (60).

The max-work Landauer efficiency η_W^L for coarse-grain measurement in the Bell basis is shown by the dashed red curve in Fig. 2. We observe that a significantly higher efficiency can be achieved with a coarse-grained measurement in the Bell basis as compared to a fine-grain measurement in the same basis. This is corroborated in Fig. 3, which shows how the total work output is larger and the information gathering cost is smaller in the coarse-grain measurement compared to the fine-grain measurement in the Bell basis, both of which contribute to the higher efficiency for the coarse-grain measurement.

E. Extra-coarse-grained measurement

We finally turn to an even further coarse-grained measurement. While the previous two examples with coarse-graining featured projector sets with two rank-1 projectors and one rank-2 projector, we now examine an extra-coarse-grained measurement featuring two rank-2 projectors. The projectors can be written in either the $\boldsymbol{E}$ or Bell basis as follows:

$$\Pi_1^E = \Pi_1^B + \Pi_3^B = E_{00} + E_{11}, \tag{64}$$

$$\Pi_2^E = \Pi_2^B + \Pi_4^B = E_{01} + E_{10}. \tag{65}$$

In words, this observable measures whether the qubits are in the same state (i.e., both in the ground state or both in the excited state) or in opposite states (i.e., one qubit in the ground state, one qubit in the excited state). Measurement will collapse the state of the system into the states

$$\rho_1^E = \frac{1}{q_{00}+q_{11}} \begin{pmatrix} q_{00} & 0 & 0 & 0 \\ 0 & 0 & 0 & 0 \\ 0 & 0 & 0 & 0 \\ 0 & 0 & 0 & q_{11} \end{pmatrix},$$

$$\rho_2^E = \frac{1}{q_{01}+q_{10}} \begin{pmatrix} 0 & 0 & 0 & 0 \\ 0 & q_{01} & 0 & 0 \\ 0 & 0 & q_{10} & 0 \\ 0 & 0 & 0 & 0 \end{pmatrix} \tag{66}$$

with probabilities $p_1^E = q_{00} + q_{11}$ and $p_2^E = q_{01} + q_{10}$, respectively, where the q_α are defined in Eq. (52). We select ergotropy unitaries to maximize total work output. Explicitly, the feedback unitaries are defined as

$$U_1^E = \begin{pmatrix} 1 & 0 & 0 & 0 \\ 0 & 0 & 0 & 1 \\ 0 & 0 & 1 & 0 \\ 0 & 1 & 0 & 0 \end{pmatrix},$$

$$U_2^E = \begin{cases} \begin{pmatrix} 0 & 0 & 1 & 0 \\ 0 & 1 & 0 & 0 \\ 1 & 0 & 0 & 0 \\ 0 & 0 & 0 & 1 \end{pmatrix} & \text{if} \quad q_{10} > q_{01} \\ \begin{pmatrix} 0 & 1 & 0 & 0 \\ 0 & 0 & 1 & 0 \\ 1 & 0 & 0 & 0 \\ 0 & 0 & 0 & 1 \end{pmatrix} & \text{if} \quad q_{01} > q_{10}. \end{cases} \tag{67}$$

Since the q_α are determined by the initial parameters of the WS, U_2^E can be defined at the outset of the problem.

We plot η_W^L for the extra-coarse-grain measurement in Fig. 2 with the dash-dot purple curve. It features interesting relationships with the efficiencies of the other measurements we have considered. Comparing the efficiency of the extra-coarse-grain measurement with those of the $\boldsymbol{E}$-basis measurements, we observe that the efficiency of the extra-coarse-grain measurement is strictly greater than that of the coarse-grain measurement, but experiences a crossover with that of the fine-grain measurement. Comparing the efficiency of the extra-coarse-grain measurement with those of the Bell-basis measurements, we observe the opposite. Namely, the efficiency of the extra-coarse-grain measurement is strictly greater than that of the fine-grain measurement, but experiences a crossover with that of the coarse-grain measurement.

The most remarkable observation emerging from Fig. 3 is that there are crossing points in the total work output curves between the coarse and extra-coarse measurements

in both bases. This reveals the intriguing fact that gathering less information will in some instances not only achieve a higher efficiency, but also achieve a higher total work output. Intuitively, one might expect that gathering less information would result in a lower total work output, since information generally aids in extracting more work. However, the total work output, Eq. (22), contains two competing terms. The first term, $\langle W\rangle_{\rm fc}^{\rm out}$, decreases with increasing coarseness (i.e., less information), thereby *decreasing* total work output. However, the second term, $\langle W\rangle_{\rm m}$, also decreases with increasing coarseness, thereby *increasing* total work output. Our plots demonstrate that depending on the system parameters, increasing coarseness may cause the benefit of decreasing the latter term to outweigh the disadvantage of decreasing the former term, thus resulting in an overall advantage (i.e., higher total work output). Interestingly, Figs. 2 and 3(c) demonstrate that there are ranges of system parameters where extra-coarse-grain measurement achieves both better total work output and efficiency compared to a moderate-coarse-grain measurement. In other words, in some scenarios, less information can be advantageous for both total work output and efficiency.

VII. DISCUSSION

Before concluding, there are a few remarks that warrant discussion. First, while we have focused on projective measurements, the theory can be extended to include generic positive operator-valued measures (POVMs). In that case the proof of Eq. (16) would be more involved, and can be achieved by following the lines of Sagawa and Ueda [26].

Second, most of our results have relied on the assumption that the thermodynamic cost incurred in the measurement process saturates the Landauer bound, Eq. (14). However, in an experimental realization, one typically expects that the actual cost will be much higher. This is because the measurement involves the displacement of a macroscopic pointer, the associated work of which would typically scale with its mass, i.e., in an extensive way. See for example Ref. [52] where this was observed in the Curie-Weiss model of quantum measurement, where the state of a spin is imprinted in the total magnetization of a ferromagnet [53,54]. This is also corroborated by Ref. [55], where the encoding of a single bit into the magnetization of a macroscopic Ising network of N superconducting qubits was experimentally observed to have a cost of the order NkT. See also the numerical study of Ref. [43]. This evidences that, in practice, the positive energy output achieved by the feedback control $\langle W\rangle_{\rm fc}^{\rm out}$ could be greatly overcome by the positive energetic cost of the measurement $\langle W\rangle_{\rm m}$ [see Eq (22)].

In order to keep the thermodynamic balance positive, it is crucial to approach the Landauer bound. However, as highlighted in Refs. [56,57], this comes at the cost of other resources, namely, either the time duration or the complexity of the measurement protocol. In order for the machine to be useful, the total time duration of the cycle should be kept finite in order to output some finite power. Thus, the cost must likely be paid in terms of complexity of the measurement protocol [56].

Third, we note that besides the timescale of measurement τ_m, there are two more relevant timescales in our theory: the timescale τ_u of the unitary driving in the first stroke, and the thermal relaxation timescale τ_r in the second stroke. The relaxation time τ_r can greatly vary from system to system, but the challenge is typically that of making it long, rather than making it short. The unitary operation timescale τ_u can similarly greatly vary from case to case. Generally, one can trade it with increased complexity of the unitary or with decreased energy output $\langle W\rangle_{\rm fc}^{\rm out}$ [57,58]. These two timescales are present as well in standard feedbackless two-stroke quantum heat engines [6,12].

Finally, we note that we have focused only on the heat engine operation regime in this work. The cooling operation regime, which is characterized by extraction of heat from the coldest bath, is also of great interest for various applications. We leave analysis of its maximal efficiency and heat extraction, along with their dependence on the choice of projectors $\mathbf{\Pi}$, for future work. Due to the high nonlinearity of the problem, we foresee a plethora of interesting phenomena and tradeoffs occurring in this regime as well.

VIII. CONCLUSION

By grounding our analysis of feedback-controlled quantum thermal machines in the explicit physical model of a two-stroke heat engine, we were able to uncover intriguing observations about the intricacy of the effect information has on the efficiency of such machines. Information has been demonstrated to augment performance of quantum engines, sometimes even endowing functionality to a system that would otherwise provide no useful output (as in the case of the Szilard engine). One might therefore conclude that more information always leads to better performance in feedback-controlled machines. However, upon analysis of explicit scenarios, we found that maximum information extraction can lead to lower efficiency, which may at first seem counterintuitive.

By placing the WS and the demon's memory on equal footing, as we do in our approach, this observation becomes more apparent in hindsight. The extracted information must be written into a memory, which is stored at some temperature T_0. There is an associated, unavoidable, work cost with storing this information, which will scale with T_0. As T_0 is independent of the bath temperatures associated with the WS, there are situations in which the cost of storing more information can outweigh the benefits of the additional work extraction this information provides. In these instances, efficiency of the engine can be improved by extracting less information (i.e., coarse-graining the measurement).

It is interesting to consider the implications of such an observation. For example, consider a very rough description for a living organism, which at a fundamental level performs measurements and decides its next action based on the information collected from the measurement. A simplified model for an organism could thus be viewed as a feedback-controlled engine. For living organisms, a key metric for survival is efficiency, as energy is a precious resource. The type of measurements an organism evolves to perform should therefore maximize the efficiency. Our results indicate that these measurements are thus not necessarily those which extract maximal information.

Coarse-graining information intake may indeed be instrumental for living organisms' survival.

Bringing the discussion back to more well-defined systems, our results have more direct and immediate applicability to design considerations for miniature devices featuring quantum thermal machines. When constructing such devices, there is not only room to optimize engine performance based on the parameters of the WS itself, but also based on the amount of information gained from measurements, which can be tuned based on the type of measurement performed (i.e., the measurement basis used, and the level of coarse-graining).

ACKNOWLEDGMENT

L.B.O. gratefully acknowledges funding from the European Union's Horizon 2020 research and innovation program under the Marie Skłodowska-Curie Grant Agreement No. 101063316.

DATA AVAILABILITY

The data that support the findings of this article are openly available [59].

APPENDIX: PROOF OF EQ. (16)

Since von Neumann information is convex and invariant under unitary transformations, using Eqs. (7) and (9), we have

$$\mathcal{H}[\rho'] \geqslant \sum_{\alpha=1}^{K} q_\alpha \mathcal{H}[\rho'_\alpha] = \sum_{\alpha=1}^{K} q_\alpha \mathcal{H}[\rho_\alpha]. \tag{A1}$$

Let us consider the density operator

$$\bar{\rho} = \sum_{\alpha=1}^{K} q_\alpha \rho_\alpha = \sum_{\alpha=1}^{K} \Pi_\alpha \rho \Pi_\alpha. \tag{A2}$$

Let $|\psi_k\rangle$ be its eigenvectors, and r_k the corresponding eigenvalues. Since $\bar{\rho}$ is block diagonal with each block represented by $q_\alpha \rho_\alpha$, its eigenbasis $\{|\psi_k\rangle, k = 1 \dots d\}$ is the union of the eigenbases $\{|\psi_k\rangle, k \in I_\alpha\}$ of the operators $q_\alpha \rho_\alpha$, spanning the according subspaces, labeled by the index α. Here I_α is the set of labels k referring to the eigenstates $|\psi_k\rangle$ spanning the α subspace. Note that the number of elements of I_α is g_α, and $\cup_\alpha I_\alpha = \{1 \dots d\}$.

The operator ρ_α is diagonal in the basis $\{|\psi_k\rangle, k \in I_\alpha\}$ with eigenvalues r_k/q_α. Thus,

$$\mathcal{H}[\rho_\alpha] = -\sum_{k \in I_\alpha} (r_k/q_\alpha) \ln(r_k/q_\alpha) \tag{A3}$$

and therefore

$$\sum_{\alpha=1}^{K} q_\alpha \mathcal{H}[\rho_\alpha] = -\sum_{\alpha=1}^{K} \sum_{k \in I_\alpha} r_k \ln r_k + \sum_{\alpha=1}^{K} \sum_{k \in I_\alpha} r_k \ln q_\alpha. \tag{A4}$$

Furthermore, $\sum_{k \in I_\alpha} r_k = \mathrm{Tr} \Pi_\alpha \rho \Pi_\alpha = q_\alpha$, and $\sum_{\alpha=1}^{K} \sum_{k \in I_\alpha} = \sum_{k=1}^{d}$, thus

$$\begin{aligned} \sum_{\alpha=1}^{K} q_\alpha \mathcal{H}[\rho_\alpha] &= -\sum_{k=1}^{d} r_k \ln r_k + \sum_{\alpha=1}^{K} q_\alpha \ln q_\alpha \\ &= \mathcal{H}[\bar{\rho}] - h[\{q_\alpha\}]. \end{aligned} \tag{A5}$$

Finally, note that the linear transformation that maps ρ onto $\bar{\rho}$, Eq. (A2), is unital. Therefore $\mathcal{H}[\bar{\rho}] \geqslant \mathcal{H}[\rho]$ [50]. Combining everything together we get

$$\mathcal{H}[\rho'] \geqslant \mathcal{H}[\bar{\rho}] - h[\{q_\alpha\}] \geqslant \mathcal{H}[\rho] - h[\{q_\alpha\}] \tag{A6}$$

which proves Eq. (16).

[1] in *Quantum Thermodynamics*, edited by J. Gemmer, M. Michel, and G. Mahler, Lecture Notes in Physics Vol. 784 (Springer-Verlag, Berlin, 2009).
[2] F. Binder, L. A. Correa, C. Gogolin, J. Anders, and G. Adesso, *Thermodynamics in the Quantum Regime: Fundamental Aspects and New Directions*, Fundamental Theories of Physics Vol. 195 (Springer, New York, 2018).
[3] S. Deffner and S. Campbell, *Quantum Thermodynamics: An Introduction to the Thermodynamics of Quantum Information* (Morgan and Claypool, San Rafael, California, USA, 2019).
[4] P. Strasberg, *Quantum Stochastic Thermodynamics Foundations and Selected Applications*, Oxford Graduate Texts (Oxford University, New York, 2022).
[5] S. Campbell, I. D'Amico, M. A. Ciampini, J. Anders, N. Ares, S. Artini, A. Auffeves, L. B. Oftelie, L. Bettman, M. V. Bonança, T. Busch, M. Campisi, M. F. Cavalcante, L. A. Correa, E. Cuestas, C. B. Dag, D. Salambô, S. Deffner, A. del Campo, A. Deutschmann-Olek, *et al.*, Roadmap on quantum thermodynamics, Quantum Sci. Technol. **11**, 012501 (2025).
[6] H.-T. Quan, Y.-X. Liu, C.-P. Sun, and F. Nori, Quantum thermodynamic cycles and quantum heat engines, Phys. Rev. E **76**, 031105 (2007).
[7] T. Denzler and E. Lutz, Efficiency fluctuations of a quantum heat engine, Phys. Rev. Res. **2**, 032062(R) (2020).
[8] A. Solfanelli, G. Giachetti, M. Campisi, S. Ruffo, and N. Defenu, Quantum heat engine with long-range advantages, New J. Phys. **25**, 033030 (2023).
[9] A. Levy and R. Kosloff, Quantum absorption refrigerator, Phys. Rev. Lett. **108**, 070604 (2012).
[10] N. Brunner, M. Huber, N. Linden, S. Popescu, R. Silva, and P. Skrzypczyk, Entanglement enhances cooling in microscopic quantum refrigerators, Phys. Rev. E **89**, 032115 (2014).
[11] R. Kosloff and A. Levy, Quantum heat engines and refrigerators: Continuous devices, Annu. Rev. Phys. Chem. **65**, 365 (2014).
[12] M. Campisi, J. Pekola, and R. Fazio, Nonequilibrium fluctuations in quantum heat engines: Theory, example, and possible solid state experiments, New J. Phys. **17**, 035012 (2015).
[13] H. Tajima and K. Funo, Superconducting-like heat current: Effective cancellation of current-dissipation trade-off by quantum coherence, Phys. Rev. Lett. **127**, 190604 (2021).
[14] S. Kamimura, H. Hakoshima, Y. Matsuzaki, K. Yoshida, and Y. Tokura, Quantum-enhanced heat engine based on superabsorption, Phys. Rev. Lett. **128**, 180602 (2022).

[15] L. M. Cangemi, C. Bhadra, and A. Levy, Quantum engines and refrigerators, Phys. Rep. **1087**, 1 (2024).
[16] J. J. Park, K.-H. Kim, T. Sagawa, and S. W. Kim, Heat engine driven by purely quantum information, Phys. Rev. Lett. **111**, 230402 (2013).
[17] K. Brandner, M. Bauer, M. T. Schmid, and U. Seifert, Coherence-enhanced efficiency of feedback-driven quantum engines, New J. Phys. **17**, 065006 (2015).
[18] C. Elouard and A. N. Jordan, Efficient quantum measurement engines, Phys. Rev. Lett. **120**, 260601 (2018).
[19] J. C. Maxwell, *Theory of Heat* (Appleton, London, 1871).
[20] L. Szilard, Über die entropieverminderung in einem thermodynamischen system bei eingriffen intelligenter wesen, Z. Phys. **53**, 840 (1929).
[21] R. Landauer, Irreversibility and heat generation in the computing process, IBM J. Res. Dev. **5**, 183 (1961).
[22] C. H. Bennett, The thermodynamics of computation—A review, Int. J. Theor. Phys. **21**, 905 (1982).
[23] S. Lloyd, Quantum-mechanical Maxwell's demon, Phys. Rev. A **56**, 3374 (1997).
[24] T. D. Kieu, The second law, Maxwell's demon, and work derivable from quantum heat engines, Phys. Rev. Lett. **93**, 140403 (2004).
[25] H. T. Quan, Y. D. Wang, Y.-X. Liu, C. P. Sun, and F. Nori, Maxwell's demon assisted thermodynamic cycle in superconducting quantum circuits, Phys. Rev. Lett. **97**, 180402 (2006).
[26] T. Sagawa and M. Ueda, Second law of thermodynamics with discrete quantum feedback control, Phys. Rev. Lett. **100**, 080403 (2008).
[27] T. Sagawa and M. Ueda, Minimal energy cost for thermodynamic information measurement and information erasure, Phys. Rev. Lett. **102**, 250602 (2009).
[28] T. Sagawa, Thermodynamics of information processing in small systems, Prog. Theor. Phys. **127**, 1 (2012).
[29] D. Mandal, H. T. Quan, and C. Jarzynski, Maxwell's refrigerator: An exactly solvable model, Phys. Rev. Lett. **111**, 030602 (2013).
[30] J. M. Parrondo, J. M. Horowitz, and T. Sagawa, Thermodynamics of information, Nat. Phys. **11**, 131 (2015).
[31] J. Goold, M. Huber, A. Riera, L. Del Rio, and P. Skrzypczyk, The role of quantum information in thermodynamics—A topical review, J. Phys. A **49**, 143001 (2016).
[32] S. Toyabe, T. Sagawa, M. Ueda, E. Muneyuki, and M. Sano, Experimental demonstration of information-to-energy conversion and validation of the generalized Jarzynski equality, Nat. Phys. **6**, 988 (2010).
[33] J. V. Koski, V. F. Maisi, J. P. Pekola, and D. V. Averin, Experimental realization of a Szilard engine with a single electron, Proc. Natl. Acad. Sci. USA **111**, 13786 (2014).
[34] P. A. Camati, J. P. S. Peterson, T. B. Batalhao, K. Micadei, A. M. Souza, R. S. Sarthour, I. S. Oliveira, and R. M. Serra, Experimental rectification of entropy production by Maxwell's demon in a quantum system, Phys. Rev. Lett. **117**, 240502 (2016).
[35] N. Cottet, S. Jezouin, L. Bretheau, P. Campagne-Ibarcq, Q. Ficheux, J. Anders, A. Auffèves, R. Azouit, P. Rouchon, and B. Huard, Observing a quantum Maxwell demon at work, Proc. Natl. Acad. Sci. USA **114**, 7561 (2017).
[36] Y. Masuyama, K. Funo, Y. Murashita, A. Noguchi, S. Kono, Y. Tabuchi, R. Yamazaki, M. Ueda, and Y. Nakamura, Information-to-work conversion by Maxwell's demon in a superconducting circuit quantum electrodynamical system, Nat. Commun. **9**, 1291 (2018).
[37] A. Kumar, T.-Y. Wu, F. Giraldo, and D. S. Weiss, Sorting ultracold atoms in a three-dimensional optical lattice in a realization of Maxwell's demon, Nature (London) **561**, 83 (2018).
[38] K. Aggarwal, A. Rolandi, Y. Yang, J. Hickie, D. Jirovec, A. Ballabio, D. Chrastina, G. Isella, M. T. Mitchison, M. Perarnau-Llobet, *et al.*, Rapid optimal work extraction from a quantum-dot information engine, Phys. Rev. Res. **7**, L032017 (2025).
[39] A. de Oliveira Junior, J. B. Brask, and R. Chaves, A friendly guide to exorcising Maxwell's demon, PRX Quantum **6**, 030201 (2025).
[40] M. Campisi, J. Pekola, and R. Fazio, Feedback-controlled heat transport in quantum devices: Theory and solid-state experimental proposal, New J. Phys. **19**, 053027 (2017).
[41] To see this, use the resolution of the identity, $\sum_{\alpha=1}^{K} \Pi_\alpha = \mathbb{I}$, and the unitarity of U, implying $UU^\dagger = \mathbb{I}$.
[42] S. Vaikuntanathan and C. Jarzynski, Modeling Maxwell's demon with a microcanonical Szilard engine, Phys. Rev. E **83**, 061120 (2011).
[43] L. Buffoni and M. Campisi, Spontaneous fluctuation-symmetry breaking and the Landauer principle, J. Stat. Phys. **186**, 31 (2022).
[44] L. Buffoni, A. Solfanelli, P. Verrucchi, A. Cuccoli, and M. Campisi, Quantum measurement cooling, Phys. Rev. Lett. **122**, 070603 (2019).
[45] A. Solfanelli, M. Falsetti, and M. Campisi, Nonadiabatic single-qubit quantum Otto engine, Phys. Rev. B **101**, 054513 (2020).
[46] M. Campisi and R. Fazio, Dissipation, correlation and lags in heat engines, J. Phys. A **49**, 345002 (2016).
[47] Similarly, in the case when the hybrid machine operates as a refrigerator, its cooling efficiency is bounded by the cooling Carnot efficiency [46].
[48] For simplicity here we adopt the convention that temperature is measured in units of energy, which is formally equivalent to setting Boltzmann constant k_B to unity.
[49] A. E. Allahverdyan, R. Balian, and Th. M. Nieuwenhuizen, Maximal work extraction from finite quantum systems, Europhys. Lett. **67**, 565 (2004).
[50] T. Sagawa, *Entropy, Divergence, and Majorization in Classical and Quantum Thermodynamics*, Springer Briefs in Mathematical Physics (Springer, New York, 2020).
[51] F. L. Curzon and B. Ahlborn, Efficiency of a Carnot engine at maximum power output, Am. J. Phys. **43**, 22 (1975).
[52] T. M. Nieuwenhuizen, Dynamics of the ideal quantum measurement of a spin-1 with a Curie-Weiss magnet, Front. Quantum Sci. Technol. **4**, 1603372 (2025).
[53] A. E. Allahverdyan, R. Balian, and T. M. Nieuwenhuizen, Curie-Weiss model of the quantum measurement process, Europhys. Lett. **61**, 452 (2003).
[54] A. E. Allahverdyan, R. Balian, and T. M. Nieuwenhuizen, Understanding quantum measurement from the solution of dynamical models, Phys. Rep. **525**, 1 (2013).
[55] L. Buffoni and M. Campisi, Cooperative quantum information erasure, Quantum **7**, 961 (2023).

[56] Y. Guryanova, N. Friis, and M. Huber, Ideal projective measurements have infinite resource costs, Quantum **4**, 222 (2020).

[57] P. Taranto, F. Bakhshinezhad, A. Bluhm, R. Silva, N. Friis, M. P. E. Lock, G. Vitagliano, F. C. Binder, T. Debarba, E. Schwarzhans, F. Clivaz, and M. Huber, Landauer versus Nernst: What is the true cost of cooling a quantum system? PRX Quantum **4**, 010332 (2023).

[58] L. Bassman Oftelie, A. De Pasquale, and M. Campisi, Dynamic cooling on contemporary quantum computers, PRX Quantum **5**, 030309 (2024).

[59] https://github.com/lebassman/Information_Engines.